

Schottky barrier and attenuation length for hot hole injection in nonepitaxial Au on *p*-type GaAs

Ilona Sitnitsky, John J. Garramone, and Joseph Abel

College of Nanoscale Science and Engineering, University at Albany, SUNY, Albany, New York 12203

Peng Xu, Steven D. Barber, Matt L. Ackerman, J. Kevin Schoelz, and Paul M. Thibado^{a)}

Department of Physics, University of Arkansas, Fayetteville, Arkansas 72701

Vincent P. LaBella^{b)}

College of Nanoscale Science and Engineering, University at Albany, SUNY, Albany, New York 12203

(Received 15 February 2012; accepted 23 June 2012; published 10 July 2012)

Ballistic electron emission microscopy (BEEM) was performed to obtain current versus bias characteristics of nonepitaxial nanometer-thick Au on *p*-type GaAs in order to accurately measure the local Schottky barrier height. Hole injection BEEM data were averaged from thousands of spectra for various Au film thicknesses and then used to determine the attenuation length of the energetic charge carriers as a function of tip bias. The authors report an increase in attenuation length at biases near the Schottky barrier, providing evidence for the existence of coherent BEEM currents in Schottky diodes. These results provide additional evidence for the conservation of the parallel momentum of charge carriers at the metal–semiconductor interface. © 2012 American Vacuum Society. [<http://dx.doi.org/10.1116/1.4734307>]

I. INTRODUCTION

Metal–semiconductor (MS) Schottky barrier diodes are vital to modern electronics. The transport of energetic charge carriers at the MS interface in nanoscale Schottky diodes is most suitably studied with ballistic electron emission microscopy (BEEM),^{1–11} a three terminal scanning tunneling microscopy (STM) and spectroscopy technique introduced in the late 1980s. In a BEEM experiment, biased charge carriers are injected into the grounded metal base of the Schottky diode, and charges that are sufficiently energetic to overcome the Schottky barrier are registered as the BEEM current. Accurate measurement of this barrier height ϕ_b is of fundamental importance for engineering devices that utilize Schottky diodes, but the task is made difficult by a sensitive dependence on spatial inhomogeneities at the MS interface. Fortunately, the BEEM tip allows the subsurface interface to be probed with atomic-scale spatial resolution, while the narrow energy distribution of the injected charge carriers results in a high energetic resolution of about 0.02 eV.¹²

In the ideal theoretical description of BEEM currents¹ it is assumed that the charge carrier's momentum parallel to the MS interface, k_{\parallel} , and its energy are both conserved. In addition, the energy and momentum distributions at the MS interface are presumed to be identical to those at injection. Attempts to confirm or disprove this model, however, have been inconclusive. For example, if the momentum distribution is narrow, a large offset is expected in the current onset for Si(111) with respect to the onset for Si(001) (Ref. 13) because at energies near the conduction band minima, the electronic structure of Si(111) does not have states available with zero parallel momentum.¹⁴ Yet, in experiments with nonepitaxial MS systems, no delayed onset^{13,14} or only a

shallow onset⁷ has been observed. Thus, one could alternatively propose that k_{\parallel} is not conserved at the interface owing to, for instance, elastic momentum randomization events.^{13,15} In fact, it is possible in this way to reproduce from theory the aforementioned similar onset biases, but such a model is in conflict with the high spatial resolution obtained by BEEM.^{3,11} Furthermore, evidence against momentum randomization has been provided by epitaxial MS systems.^{16,17} In addition, recent BEEM hot electron attenuation length measurements on Ag/Si Schottky diodes have demonstrated that attenuation length measurements are highly sensitive to parallel momentum conservation and interface band structure effects.¹⁸ In these experiments an increase in the attenuation length was observed for tip biases near the threshold on Si(001) but *not* on Si(111) due to the lack of $k_{\parallel} = 0$ states in the Si(111) interface Brillouin zone.

In this article we present BEEM measurements of ϕ_b for nonepitaxial Au on *p*-type GaAs. Au/GaAs has been extensively studied as a prototype for nonepitaxial metal interfaces on direct bandgap semiconductors. Our technique uses an automated scanning system that allows for a large number of local measurements to be taken across the sample surface and averaged. In addition, the attenuation length λ of the energetic charge carriers is measured by varying the Au thickness, which provides insight into charge transport through the diode. A sharp increase in the observed λ as tip biases approach ϕ_b indicates that k_{\parallel} is likely conserved in charge transport across the MS interface, in accordance with the recent results from similar experiments using Ag on *n*-type Si.

II. EXPERIMENT

The GaAs sample was prepared in a liquid-nitrogen cooled, ultrahigh vacuum ($\sim 3 \times 10^{10}$ mbar) molecular beam epitaxy (MBE) growth chamber (Riber 32), which includes a

^{a)}Electronic mail: thibado@uark.edu

^{b)}Electronic mail: vlabella@albany.edu

dual Ga effusion cell, a two-zone As valved-cracker cell, and a reflection high-energy electron diffraction (RHEED) system operating at 15 keV. A commercially available, “epiready,” 2 in. diameter, $p+$ (Zn-doped 10^{19} cm^{-3}) GaAs(001) $\pm 0.1^\circ$ wafer was indium mounted on a 2 in. diameter, standard MBE molybdenum block and loaded into the MBE chamber without chemical cleaning. To remove the surface oxide layer, the substrate was heated to 580°C while exposing the surface to 10^{-5} mbar As_4 . Before growth, the Ga and As_4 beam equivalent pressures were set and measured to give an As_4/Ga flux ratio of 10. The substrate temperature was then maintained at 580°C , and GaAs was grown for 4 h. RHEED oscillations determined the growth rate of GaAs to be about $1.3 \mu\text{m}/\text{h}$, giving a final sample thickness of about $5 \mu\text{m}$. Although the film was undoped, MBE-grown GaAs films are slightly p type due to As antisite defects ($\sim 10^{15} \text{ cm}^{-3}$).¹⁹ Following growth, the chamber was cooled, and the GaAs sample was removed from the chamber and transferred to our metals deposition facility to create Schottky diodes.

Gold films of 19, 21, and 24 nm thickness were deposited through a 1 mm^2 shadow mask using a Varian electron-beam deposition system with a base pressure of 10^{-7} mbar. More thicknesses were attempted; however, thinner Au did not result in a continuous film, and thicker gold resulted in BEEM currents that were too small. After deposition, the sample was mounted onto a custom designed sample holder for BEEM measurements that allowed for simultaneous grounding of the metal film using a BeCu contact and connection of the GaAs to the *ex situ* picoammeter to measure the BEEM current. The Ohmic contact to the GaAs was fabricated by cold pressing indium into the back side of the GaAs wafer.

A modified low temperature, ultrahigh vacuum STM (Omicron) with a pressure in the 10^{-11} mbar range was utilized for all BEEM measurements.²⁰ The samples were inserted into the chamber and loaded onto the STM stage that was cooled to 80 K for all BEEM measurements. Au STM tips that were mechanically cut at a steep angle were utilized for all measurements. For each sample, BEEM spectra were acquired from thousands of unique locations throughout a $3 \mu\text{m} \times 3 \mu\text{m}$ area of the metal surface, using positive (hot hole injection) tip biasing conditions and a constant tunneling current set point of 5.0 nA. The BEEM spectra were then averaged to reduce the effects of surface roughness, which was determined to be about 1 nm from the STM images. The thickness of the metal films was determined *ex situ* by Rutherford backscattering spectrometry measurements.

For BEEM measurements with hole injection, which is much less common than electron injection, the tip is positively biased while the Au is held at ground, as shown schematically in Fig. 1(a). As in STM, the tip can move in three dimensions, and the current through the tip is monitored as it injects holes into the Au. Simultaneously, a picoammeter connected to the GaAs measures the BEEM current, which has crossed the MS interface. An energy diagram illustrating the hot hole injection process is shown schematically in Fig. 1(b). The tip and the Au are separated by a vacuum barrier, which is typically modeled as a trapezoid. A positive bias is applied to the STM tip, lowering its Fermi energy an amount

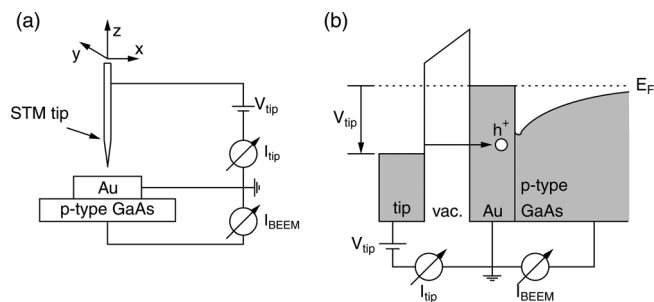


FIG. 1. (a) Schematic for the BEEM experimental setup for hot hole injection into Au on p -type GaAs. A special BeCu point contact is made to the Au film, while an indium contact was made to the GaAs using a cold press technique. (b) The corresponding energy diagram, illustrating the tip bias, hole injection, and band bending in the GaAs. A hole with sufficient energy to pass under the Schottky barrier before rising up to the Fermi level is shown.

V_{tip} below that of the grounded Au film. Thus, holes in the STM tip are injected into the metal. The semiconductor is p type, so its valence band starts out just below the Fermi level. At the MS interface, however, the valence band maximum bends below the potential of the metal, forming a Schottky barrier and creating a barrier to hot hole injection.

III. RESULTS

The BEEM spectra for the three different Au film thicknesses are shown in Fig. 2. While their shapes are similar, the overall magnitude of the BEEM current clearly decreases as the thickness of the Au layer increases. Each spectrum begins at a tip bias of -2.0 eV , where the hole transmission rate is $\sim 1\%$ for the 19 nm film, $\sim 0.3\%$ for 22 nm, and

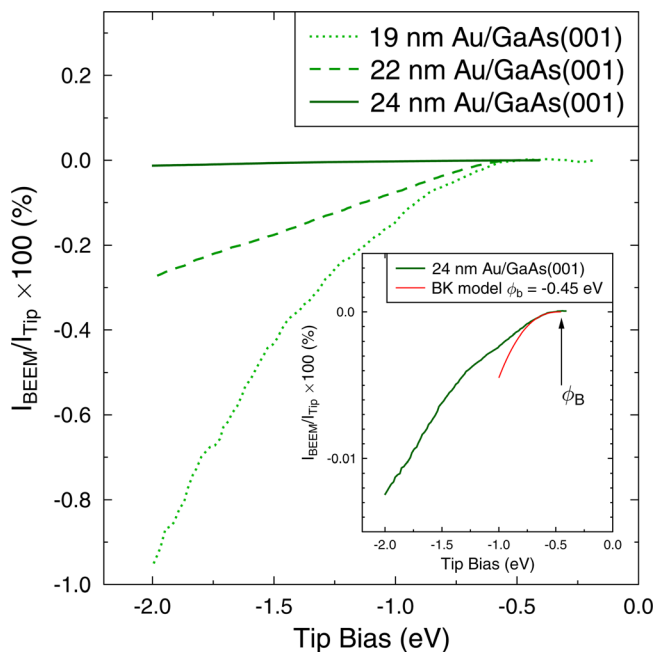


FIG. 2. (Color online) BEEM spectra showing percent transmission of the BEEM current divided by the tip current is shown vs tip bias for three different Au film thicknesses. Spectra were obtained with the STM feedback on to keep the tip current constant at 5 nA. The inset magnifies the curve associated with the 24 nm Au layer. The label just below the curve points to the tip bias at which the onset of the BEEM current is found.

$\sim 0.013\%$ for 24 nm. As the tip bias approaches zero, the transmission also monotonically decreases to zero. The inset in the lower right-hand corner of the graph magnifies the 24 nm curve to better reveal its form. The Schottky barrier height, ϕ_b , is marked on this spectrum at -0.45 eV.

For five characteristic tip biases close to ϕ_b , the absolute value of the percent transmission ($I_{\text{BEEM}}/I_{\text{tip}} \times 100$) is plotted as a function of the Au film thickness in Fig. 3. A log scale is used on the y axis, and a linear fit is applied to each data set. Each line is labeled with its corresponding tip bias, as well as the magnitude of its inverse slope, known as the attenuation length λ . Two noteworthy features of this plot are that the percent transmission decreases with increasing Au thickness, and that the slope decreases (λ increases) with increasing bias.

The attenuation length is plotted for all tip biases in Fig. 4. It starts at approximately 1.1 nm for a tip bias of -2.0 eV and slowly grows to about 1.3 nm at -0.8 eV, then rapidly increases, reaching 8.0 nm at the Schottky barrier height, -0.45 eV. The energy diagram of a hole being injected directly at the top of the Schottky barrier is displayed as an inset in the center of Fig. 4. As before, the Fermi energy of the Au is shown as a dashed line across the diagram, and the valence band maximum in the GaAs bends below the Fermi level at the MS interface. However, the tip bias has been adjusted to equal ϕ_b so that the injected hole depicted in this illustration is at the height of the valence band as it contacts the MS interface.

IV. DISCUSSION

The energy level schematic shown in Fig. 1(b) helps to understand this experiment. The difference between the

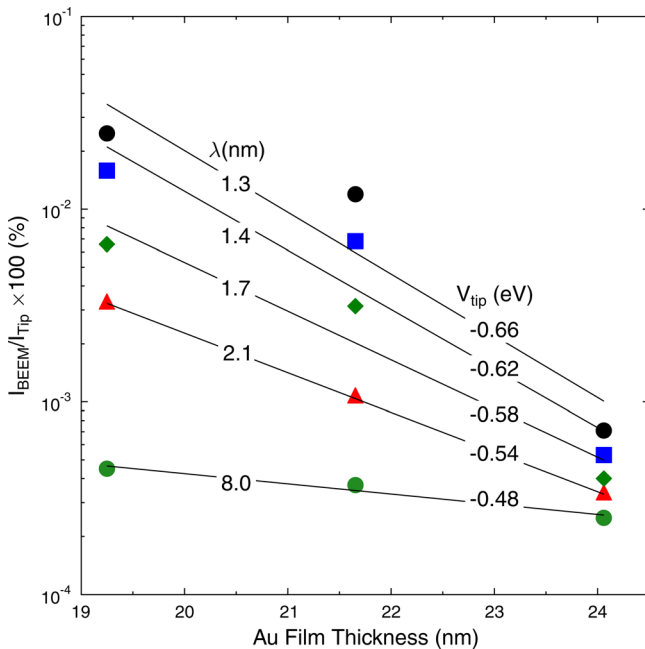


FIG. 3. (Color online) Percent transmission as a function of Au thickness plotted on a semilog scale for four tip biases close to the Schottky barrier height. Solid lines are fits to Eq. (1), where the corresponding attenuation lengths and tip biases are indicated.

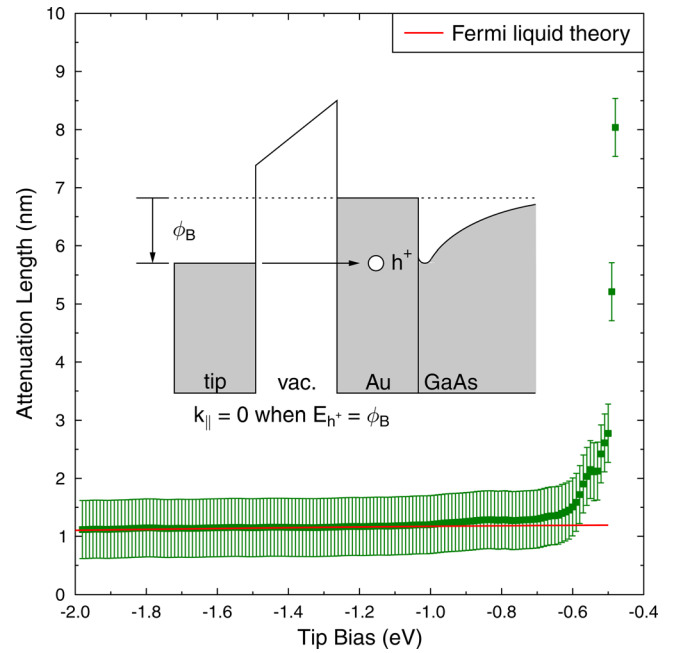


FIG. 4. (Color online) Hot hole attenuation length vs tip bias. A dramatic increase is seen as the bias approaches ϕ_b . The uncertainty in the measured attenuation length is about 1 nm. The inset shows a potential diagram for a hole injected into the diode directly at the Schottky barrier height.

Fermi level and the top of the GaAs valence band at the interface is defined as ϕ_b . A positive bias placed on the tip lowers the energy of the injected holes below the Fermi level of the grounded Au film, but only as this bias is increased past ϕ_b will some holes be sufficiently energetic to cross the barrier into the semiconductor, registering as the BEEM current I_{BEEM} . Thus, the Schottky barrier could be estimated from the spectra in Fig. 2 by simply noting the tip bias at which there is an onset of I_{BEEM} . More rigorously, it may be ascertained by fitting the curves to $I_{\text{BEEM}}/I_{\text{tip}} \propto (|V_{\text{tip}}| - \phi_b)^{5/2}$, where I_{tip} is the tunneling current^{1,21} Using this method, ϕ_b was determined to be -0.45 ± 0.02 eV for Au/p GaAs at 80 K.

The points represented in Fig. 3 can be extracted from Fig. 2 by drawing vertical lines through the spectra at the four chosen tip biases. Unsurprisingly, the percent transmission is found to decrease with increasing Au thickness due to an increased probability of scattering in the metal film. Each data set at a given tip bias individually was fit to

$$I_{\text{BEEM}}/I_{\text{tip}} \propto \exp[-d/\lambda(E, T)], \quad (1)$$

where $\lambda(E, T)$ is the hot hole attenuation length, d is the deposited film thickness, T is the temperature, and E is the energy of the charge carrier.⁸ The slope of the resulting line is inversely proportional to λ , and the decreasing slopes as the bias approaches ϕ_b must indicate an increase in λ . The surprisingly sharp nature of this increase can be seen with λ plotted versus tip bias, as in Fig. 4. At higher negative biases, λ is relatively constant and equal to approximately 1.1 nm. Between -0.7 and -0.48 eV, however, λ more than doubles, increasing to a maximum of 8 nm. We estimate the uncertainty in λ to be about 1 nm, which is close to the rms

roughness of the film and therefore the increase near the Schottky barrier height is statistically significant for this data set.

The relative contributions of elastic, λ_e , and inelastic, λ_i , scattering of the charge carriers are extracted by simultaneously fitting the data to the following Fermi liquid based model:

$$\lambda(E) = \left(\frac{1}{\lambda_i(E)} + \frac{1}{\lambda_e} \right)^{-1} = \left(\frac{E^2}{A(|E| + E_F)^{0.5}} + \frac{1}{\lambda_e} \right)^{-1}, \quad (2)$$

where E is the carrier energy (tip bias),²² E_F is the Fermi energy of the metal ($E_F^{\text{Au}} = 5.5$ eV), A is a fitting parameter, and λ_e is the elastic attenuation length.⁹ This fit is displayed as the solid line in Fig. 4 with $\lambda_e = 1.2$ nm and $A = 0.05$. The values for λ are similar to those measured on n -type GaAs(001).²³

The sharp increase and the divergence of λ from the fit to Eq. (2) as the bias approaches ϕ_b is a surprising result and similar to what has recently been observed for BEEM hot electron attenuation length measurements of silver.¹⁸ This effect results from parallel momentum k_{\parallel} conservation that filters the hot carriers so only forward focused $k_{\parallel} = 0$ carriers can traverse the barrier at low biases. This description assumes that hot carriers that arrive at the interface with $k_{\parallel} = 0$ have not scattered at the same rate as others and creates a BEEM current that is less sensitive to thickness dependent scattering in the metal. It should be noted that since holes are being injected into the valence band of GaAs there will be states available at Γ with $k_{\parallel} = 0$, in the (001) face of GaAs Brillouin zone allowing transport of the $k_{\parallel} \approx 0$ carriers.

These forward focused hot carriers are a very tiny fraction of the entire current and persist at all energies, but are quickly drowned out at higher energies from the exponential increase in the BEEM current. This exponential increase arises from elastically scattered carriers being able to traverse the barrier, which creates a BEEM current that is more sensitive to thickness dependent scattering in the metal and reduces the measured λ . It is highly likely that these carriers do not conserve parallel momentum since the acceptance cone does not broaden quickly enough to account for the sharp decrease in λ that is observed. In other words, it appears that k_{\parallel} conservation is only happening in a narrow energy range above the Schottky barrier and must be quickly suppressed by momentum randomization events at the interface. This latter observation is consistent with what has been observed over the past several decades with similar thresholds measured by BEEM on Si(001) vs Si(111) substrates. This means that in BEEM measurements there exists a tiny fraction of hot carriers that travel truly ballistically through these polycrystalline metal films and arrive at the interface unscattered. The attenuation length is highly sensitive to these carriers since it is a measure of the rate of change of the current with metal thickness.

V. CONCLUSION

In conclusion, BEEM experiments were performed on custom-made nanoscale Au/GaAs(001) p -type diodes. The Schottky barrier height for hot hole injection into p -type GaAs with Au contacts was determined to be -0.45 ± 0.02 eV at 80 K. A prominent increase in the attenuation length of the charge carriers for tip biases near ϕ_b provides evidence that the BEEM current is sensitive to the effects of parallel momentum conservation and that hot electron attenuation length measurements are a sensitive technique to study this effect.

ACKNOWLEDGMENTS

The Albany group is thankful for the support of the Interconnect Focus Center, one of five research centers funded under the Focus Center Research Program, a DARPA and Semiconductor Research Corporation program. The Arkansas group gratefully acknowledges support from the National Science Foundation (NSF) under Grant No. DMR-0855358 and the Office of Naval Research (ONR) under Grant No. N00014-10-1-0181. Experimental work was performed while I.S. was enrolled as a student at the University at Albany.

¹L. D. Bell and W. J. Kaiser, *Phys. Rev. Lett.* **61**, 2368 (1988).

²W. J. Kaiser and L. D. Bell, *Phys. Rev. Lett.* **60**, 1406 (1988).

³M. K. Weilmeyer, W. H. Rippard, and R. A. Buhrman, *Phys. Rev. B* **59**, R2521 (1999).

⁴M. K. Weilmeyer, W. H. Rippard, and R. A. Buhrman, *Phys. Rev. B* **61**, 7161 (2000).

⁵W. J. Kaiser, M. H. Hecht, R. W. Fathauer, L. D. Bell, E. Y. Lee, and L. C. Davis, *Phys. Rev. B* **44**, 6546 (1991).

⁶H. Siringhaus, T. Meyer, E. Y. Lee, and H. von Känel, *Phys. Rev. B* **53**, 15944 (1996).

⁷C. A. Bobisch, A. Bannani, Y. M. Koroteev, G. Bihlmayer, E. V. Chulkov, and R. Moller, *Phys. Rev. Lett.* **102**, 136807 (2009).

⁸C. A. Ventrice, Jr., V. P. LaBella, G. Ramaswamy, H. P. Yu, and L. J. Schowalter, *Phys. Rev. B* **53**, 3952 (1996).

⁹J. J. Garramone, J. R. Abel, I. L. Sitnitsky, L. Zhao, I. Appelbaum, and V. P. LaBella, *Appl. Phys. Lett.* **96**, 062105 (2010).

¹⁰H. J. Im, B. Kaczer, J. P. Pelz, and W. J. Choyke, *Appl. Phys. Lett.* **72**, 839 (1998).

¹¹C. Tivarus, J. P. Pelz, M. K. Hudait, and S. A. Ringel, *Phys. Rev. Lett.* **94**, 206803 (2005).

¹²M. Prietsch, *Phys. Rep.* **253**, 163 (1995).

¹³D. L. Smith, E. Y. Lee, and V. Narayanamurti, *Phys. Rev. Lett.* **80**, 2433 (1998).

¹⁴L. J. Schowalter and E. Y. Lee, *Phys. Rev. B* **43**, 9308 (1991).

¹⁵I. Appelbaum and V. Narayanamurti, *Phys. Rev. B* **71**, 045320 (2005).

¹⁶S. Guézo, P. Turban, S. DiMatteo, P. Schieffer, S. LeGall, B. Lépine, C. Lallaizon, and G. Jézéquel, *Phys. Rev. B* **81**, 085319 (2010).

¹⁷S. Parui, J. R. R. van der Ploeg, K. G. Rana, and T. Banerjee, *Phys. Status Solidi (RRL)* **5**, 388 (2011).

¹⁸J. J. Garramone, J. R. Abel, S. Barraza-Lopez, and V. P. LaBella, *Appl. Phys. Lett.* **100**, 252102 (2012).

¹⁹R. J. Wagner, J. J. Krebs, H. Stauss, and A. M. White, *Solid State Commun.* **36**, 15 (1980).

²⁰M. Krause, A. Stollenwerk, C. Awo-Affouda, B. Maclean, and V. P. LaBella, *J. Vac. Sci. Technol. B* **23**, 1684 (2005).

²¹M. Prietsch and R. Ludeke, *Phys. Rev. Lett.* **66**, 2511 (1991).

²²The carrier energy is approximated as being equivalent to the tip bias because of the exponential dependence of the tunneling distribution.

²³A. J. Stollenwerk, E. J. Spadafora, J. J. Garramone, R. J. Matyi, R. L. Moore, and V. P. LaBella, *Phys. Rev. B* **77**, 033416 (2008).